JMATPRO	Journal of Advanced Materials and Processing 11 (1): 49-60, Winter 2023 http://sanad.iau.ir/journal/jmatpro doi:10.71670/jmatpro.2024.981528

Research Paper

Thymus Carmanicus Mediated Synthesis of Zero Valent Iron Nanoparticles at Alkaline pH and Studies on Their Antibacterial Activity

Mojtaba Nasr-Esfahani[1*], Marzieh Esfahanian[2], Ali Albar Karimian[2]

1. Department of Chemistry, Najafabad Branch, Islamic Azad University, Najafabad, Iran.

2. Department of Natural Resources and Desert Studies, Yazd University, Yazd, Iran.

ARTICLE INFO

Article history:

Received 27 June 2023
Accepted 24 October 2023
Available online 1 February 2023

Keywords:
Plant-mediated Synthesis
Thymus carmanicus
Zero Valent Iron
Nanoparticle.

ABSTRACT

There are many methods to synthesize metal and metal oxide nanoparticles (NPs) using different reducing agents which are hazardous in nature. Although some researchers have used biobased materials for the synthesis of these NPs, further research is needed in this area. To explore the scope of bio-extract for the synthesis of transition metal NPs, the present paper synthesizes metal NPs replacing hazardous traditional reducing agents. This paper reports the synthesis zero-valent iron nanoparticles (ZVINs) by a green method and investigates the antibacterial activity of these nanoparticles through the extract of *Thymus carmanicus*. Green synthesis of *Thymus carmanicu*-Zero Valent Iron Nanoparticles (TC-ZVINs) was carried out in an alkaline environment. The TC-ZVINs were characterized by the use of imaging FESEM and spectroscopic (FTIR and XRD) methods. The TC-ZVINs obtained were a mixture of spherical and quasi-spherical shapes with diameters ranging between 40 and 80 nm. These methods demonstrated that some polyphenols are bound to the surfaces of the TC-ZVINs as a capping/stabilizing agent. Furthermore, The TC-ZVINs, TC extract and different percentages of them have the potential to terminate the pathogenicity of gram-negative (*Escherichia coli)* and gram-positive (*Staphylococcus aureus*) bacteria. This property is slightly higher in the TC-ZVINs than in *T. carmanicus* extract. For both types of bacteria, the diameter of the inhibitory zone obtained from TC-ZVINs was about 10.8 .

Citation: Nasr-Esfahani, M.; Esfahanian, M.; Albar Karimian, A. (2023). Thymus Carmanicus Mediated Synthesis of Zero Valent Iron Nanoparticles at Alkaline pH and Studies on Their Antibacterial Activity, Journal of Advanced Materials and Processing, 11 (1), 49-60. doi:10.71670/jmatpro.2024.981528.

Copyrights:
Copyright for this article is retained by the author (s), with publication rights granded to Journal of Advanced Materials and Processing. This is an open – acsses article distributed under the terms of the Creative Commons Attribution License (http://creativecommons.org/licenses/by/4.0), which permits unrestricted use, distribution and reproduction in any medium, provided the original work is properly cited.

[*] **Corresponding Author:**
E-Mail: mnstd@yahoo.com

1. Introduction

Nanoparticle biosynthesis is a common point among nanotechnology, natural resources, environment, and agriculture that has led to the production of widely used materials in many fields [1]. Silver nanoparticles, magnetic iron oxide, titanium dioxide, zinc oxide, and copper oxide are important materials that have been studied and can be synthesized using physical, chemical, and biological methods. In recent years, the method of biosynthesis using plant extracts has received more attention than physical and chemical methods [2,3]. The use of green plants for the biological production of nanoparticles has created a tremendous possibility and is well known [4]. Therefore, plants and plant products have been given much more attention by researchers in order to produce nanoparticles. In addition, nanoparticles produced by medicinal plants with less risk can be used in cases such as drug delivery. Studies have also shown the nanoparticles made by plants are faster and more stable than nanoparticles produced by other organisms [5]. The shape and size of nanoparticles made by plants are different from nanoparticles produced by other organisms. Therefore, the advantage of plant production of nanoparticles over other biological methods, such as the use of bacteria, algae, yeasts, and fungi, is the reliability and safety of plant methods, which are healthier, cheaper, and renewable [6]. Recently, zero-valent iron nanoparticles have been introduced as a desirable and highly effective technology for the removal of various metal ions, including lead (II), cadmium (II), arsenic (V), and chromium (VI) in aqueous solutions [7]. Nano zero-valent iron has been considered due to its cost-effective and relatively eco-friendly (low toxicity) [8]. Nanotechnology offers new solutions for the treatment of surface waters, groundwaters, and wastewaters contaminated with toxic metal ions, minerals, organics, and microorganisms through particulates and filter systems that can eliminate or inactivate air, water, and soil pollutants [9]. Zero-valent iron nanoparticles are also used for the successful treatment of various metal ions in aqueous solution [9].

Many researches have been done on the use of plants for the synthesis of iron nanoparticles. For example, Lohrasbi et al. [10] performed the green synthesis of iron nanoparticles using Plantago major leaf extract in their studies and achieved satisfactory results. Huang et al. [11] specified that polyphenols/caffeine in tea extracts acted as both reducing and capping agents that reduced the aggregation of Fe NPs and improved the stability and, in turn reactivity of Fe NPs. Devatha et al. [12] carried out the green synthesis of iron nanoparticles using different leaf extracts of Mangifera indica, Murraya Koenigii, Azadiracta indica, Magnolia champacafor and to check its potential for treating domestic wastewater. They confirmed the formation and presence of iron nanoparticles and biomolecules, which could help in capping the nanoparticles, and the overall performance of Azadiracta indica synthesized iron nanoparticles showed satisfactory results compared to other leaf extracts for treating domestic wastewater.

Many plant extracts could be an alternative to existing chemical and physical techniques for the synthesis of nanoparticles. Thymus carmanicus is a perennial dwarf shrub and endemic species to Iran [13], and numerous studies have been reported on essential oil composition, antioxidant, antibacterial, and antifungal activity. Phenolic and flavonoid compounds have been known as natural products with high antioxidant activity. Sarfaraz et al. [14] evaluated the polyphenolic profile of Thymus carmanicus using chromatography based analysis. Major phenolic and flavonoid compounds of T. *carmanicus* (in mg/100 g of sample dry weight) based on HPLC analysis were included rosmarinic acid (88.0 mg), caffeic acid (27.4 mg), salvianolic acid (23.7 mg), ferulic acid (14.2 mg). To our knowledge, the present research is the first study conducted to investigate the ability of green synthesized iron nanoparticles by T. *carmanicus* extract. However, other thymes have been used in the synthesis of nanoparticles [15, 16]. The aim of the present study was: 1) to synthesize zero-valent iron using T. *carmanicus* extract to benefit from the properties of plants and provide an eco-friendly synthesis, and 2) to study its antibacterial properties. The application of T. *carmanicus* is of interest not only for synthesizing iron nanoparticles but also for preventing the disorders associated with the resulting nanoparticle-mediated oxidative stress. Overall, the use of natural products for greener synthesis of nanoparticles/ nanomaterials is an emerging and exciting area of nanotechnology and may have a significant direct impact on further advances in biotechnology.

2. Materials and methods

2.1 Plant material and leaf extract preparation

Authenticated leaves of *T. carmanicus* were gathered from the surrounding plains of Kashan, Isfahan, Iran. The third author authenticated the plant. The dried sample was powdered and used for further studies. 50 g of the leaf powder was extracted at room temperature through the maceration method using 500 ml of ethanol [17]. The obtained extract was filtered and concentrated in a rotary vacuum until a crude extract with a yield of ~2.16% was achieved and kept at 4 °C until used for further work.

2.2. Green bio-synthesis of zero valent iron nanoparticles (TC-ZVINs)

The stabilized zero-valent iron (ZVIN) was prepared by reducing Fe^{3+} to Fe^0 using *T. carmanicus* extract and ascorbic acid as an antioxidant agent to protect the iron (III) ions from oxidation without air evacuation. The synthesis process is based on the following: 0.4 g of sodium hydroxide was added to 50 ml of the extract solution. 1.4 g of Fe^{3+} chloride and 0.9 g of ascorbic acid were mixed in 50 ml of water and alcohol solution with a volume ratio of 30:70. An extract solution with NaOH was poured into a burette and added drop by drop to this solution at a volume ratio of 2:1 with strenuous shaking. The change in color of the iron chloride solution from pale yellow to brown and then black suggested the reduction of iron ions. The stirring was continued for another 30 minutes to complete the reaction. The TC-ZVINs achieved were centrifuged at 14000 rpm for 20 minutes and then washed three times using deionised water and ethanol to eliminate any unreacted biomolecules. As a positive control, Zero-valent iron synthesized using sodium borohydrate (SB-ZVIN) was also prepared for comparison.

2.3. Synthesis of zero iron using sodium borohydride (SB-ZVINs)

The reduction reaction with sodium borohydride is reported in the literature [18-20]. The SB-ZVIN was prepared in cold distilled water by reducing Fe^{3+} to Fe^0 in the presence of ascorbic acid as a reducing agent to stabilize ZVIN without air evacuation. In this approach, the SB-ZVIN were synthesized by $NaBH_4$ reduction method without application of inert gas according to the following reaction:

$$4Fe^{3+}+3BH_4^-+9H_2O\rightarrow 4Fe^0\downarrow+3H_2BO_3^-+12H^++6H_2 \quad (1)$$

Typically, 1:1 volume ratio of $NaBH_4$ (0.2 M) and $FeCl_3\cdot 6\text{-}\ H_2O$ (0.05 M) were vigorously mixed in the flask reactor for additional 30 min after the titration. The generated iron particles were harvested with vacuum filtration and stabilized with a large volume of deionized water (> 100 mL/g) to wash and, in the end, with diluted ethanol (~5%). For storage, our experience suggests that maintaining a thin layer of ethanol on top of iron particles can help preserve the nanoparticles.

2.4. Characterization of nanoparticles

X-Ray Diffraction (XRD): Purified iron and iron NPs were subjected to X-ray diffraction analysis (Philips X' pert 1066 MPD system, λ= 1.542 Aº) for checking the crystallinity of NPs. The scanning range was done between 10 and 90º.

Fourier Transformed Infrared Spectroscopy (FTIR): Purified iron and iron NPs were then analyzed using FT-IR spectral measurements to identify the possible biomolecules responsible for the reduction and capping/stabilizing of NPs. The measurements were carried out on an FT-IR-6300, JASCO, Japan instrument in the range of 400-4000 cm^{-1} with a scanning rate of 2 cm^{-1}.

Field Emission Scanning Electron Microscope (FESEM): The surface morphology and grain size of the zero-valent iron sample prepared by field emission scanning electron microscope (Mira III model manufactured by Tescan, Czech Republic) at an operating voltage of 5 to 25 kV were examined.

2.5. Antibacterial activity by disc diffusion method

Anti-bacterial activity was done on two standard strains of Gram-negative *Escherichia coli* and Gram-positive *Staphylococcus aureus* prepared from the Mushroom and Bacteria Collection Center of Iran by the standard disc diffusion method. Merck company media were used to grow and maintain the bacteria. A combination of percentages containing 0, 20, 40, 60, 80, and 100% of TC extracts and the TC-ZVINs was prepared. 0.04 g of each sample was mixed with 5 µl of DMSO. The discs were air-dried in a sterile condition. Nutrient agar (NA) plates were seeded with 8 h broth culture of different bacteria. Using sterilized dropping pipettes, 5 µl of the samples were applied on the paper discs (the disc diameter was 6 mm). Then, disc papers were placed in the inoculated plates. After 24 h of incubation at 37 °C the diameter of growth inhibition zones was measured [21].

2.5.2. Statistical analyses

All the experiments were done in triplicates, and the results were expressed as Mean ± SD. The data were statistically analyzed using one-way ANOVA followed by Duncan's test. Mean values were considered statistically significant when $p>0.05$.

3. Results and discussion

3.1. Synthesis of iron nanoparticles

Fig. 1 shows a schematic illustration of *T. carmanicus* mediated synthesis of ZVINs. On adding ferric chloride solution to the aqueous *T. carmanicus* extracts, the solutions instantaneously turned from pale yellow to dark brownish, indicating the formation of iron nanoparticles and the first step in identifying the process of biosynthesis [22]. The discoloration of the iron chloride solution in the presence of *T. carmanicus* extract was observed. Nanoparticles turn black due to the stimulation of surface plasmon vibrations [9], which is a good tool for detecting the formation of iron nanoparticles in the environment. Sedimentation was not observed after a week of storage. This suggests that the synthesized iron nanoparticles were stabilized by the polyphenols in the *T. carmanicus* extract.

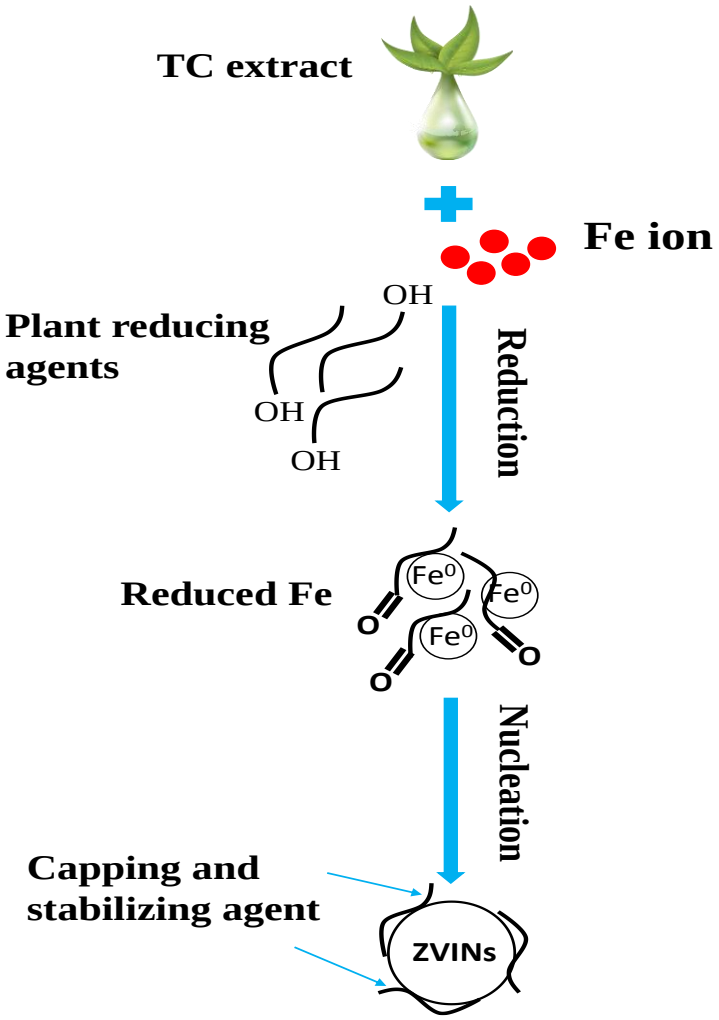

Fig. 1. Schematic illustration of T. carmanicus-mediated synthesis of ZVINs

Green synthesis of nanoparticles using T. *carmanicus* aerial part extract is an example of the formation of zero-valent iron nanoparticles that have been used as an antioxidant to protect Fe^{3+} ions from oxidation in the presence of air. As mentioned, the phenolic and hydroxyl groups in the extract give the properties of a good coating agent to stabilize the active surfaces of the nanoparticles and also reduce the biotoxicity of the nanoparticles produced [23]. In all plants, antioxidant activity is directly related to the amount of phenolic and flavonoid compounds [24]. In this study, we synthesized the TC-ZVINs in an alkaline environment and afterward assessed the antioxidant characteristics of the resulting nanoparticles. In the alkaline environment, the hydroxyl and carboxylic groups of polyphenolic compounds contained in the *T. carmanicus* extract are deprotonated and are made stronger as a complexing and reducing agent for the iron ions. Subsequently, the iron ions oxidized the hydroxyl groups into carbonyl groups in the reduction reaction as the iron ions were concurrently reduced into the ZVINs. Multiple investigations have recently indicated that an alkaline medium is a precondition for synthesizing metallic nanoparticles using active reducing components from bio-resources [25, 26]. Polyphenolic compounds in *T. carmanicus* hydroalcoholic extract (mainly rosmarinic and caffeic acid) act as both reducing and coating/stabilizing agents for this synthesis.

3.2. X-ray Diffraction (XRD)

XRD is one of the efficient techniques in nanomaterial analysis. The crystalline nature of the particles can be understood using XRD analysis and its output patterns. However, the particle size can also be estimated using this device. The XRD pattern of zero iron nanoparticles obtained by chemical method (SB-ZVIN) is shown in Fig. 2a indicating that the zero-valent iron has only a characteristic 2θ value of 44.7°, and no signals for iron oxides with a 2θ value of 36° were found. It also indicates that the ZVI is mainly seen in the sample. The XRD pattern of zero iron nanoparticles obtained by biosynthesis method using *T. carmanicus* extract (TC-ZVINs) is shown in Fig. 2b. From the XRD pattern, it may be noted that there is no such strong distinctive diffraction pattern suggesting that the as prepared NPs are purely amorphous in nature. Organic coating due to polyphenolic compounds has weakened the XRD pattern of ZVI NPs [27]. A deeper look at the pattern

reveals the appearance of two broad peaks in the region 2θ = 24–25° and 2θ = 43–44°. The broad hump shoulder peak at 2θ = 24–25° is identified as organic compounds (phenolic compounds of *T. carmanicus*) adsorbed from the extract as reducing or capping or stabilizing agent [28-30]. More precisely peak at 2θ = 43.6° in the region 2θ = 43–44° corresponds to the presence of ZVI [31] which matched very well with the JCPDS Card No. 01-087-0722. Traces of oxides of iron might be present as the phenolic compounds present in the extract might have got partially oxidized during synthesis. Correlating our work with the recently published reports, it is now inferred that green synthesized iron NPs contain mainly zero-valent iron [32, 33]. The size of the crystals obtained by the Scherrer method for the SB-ZVINs and the TC-ZVINs were about 10 and 7 nm, respectively, which can indicate the formation of smaller crystals using the biosynthesis method and thus the use of plant extracts.

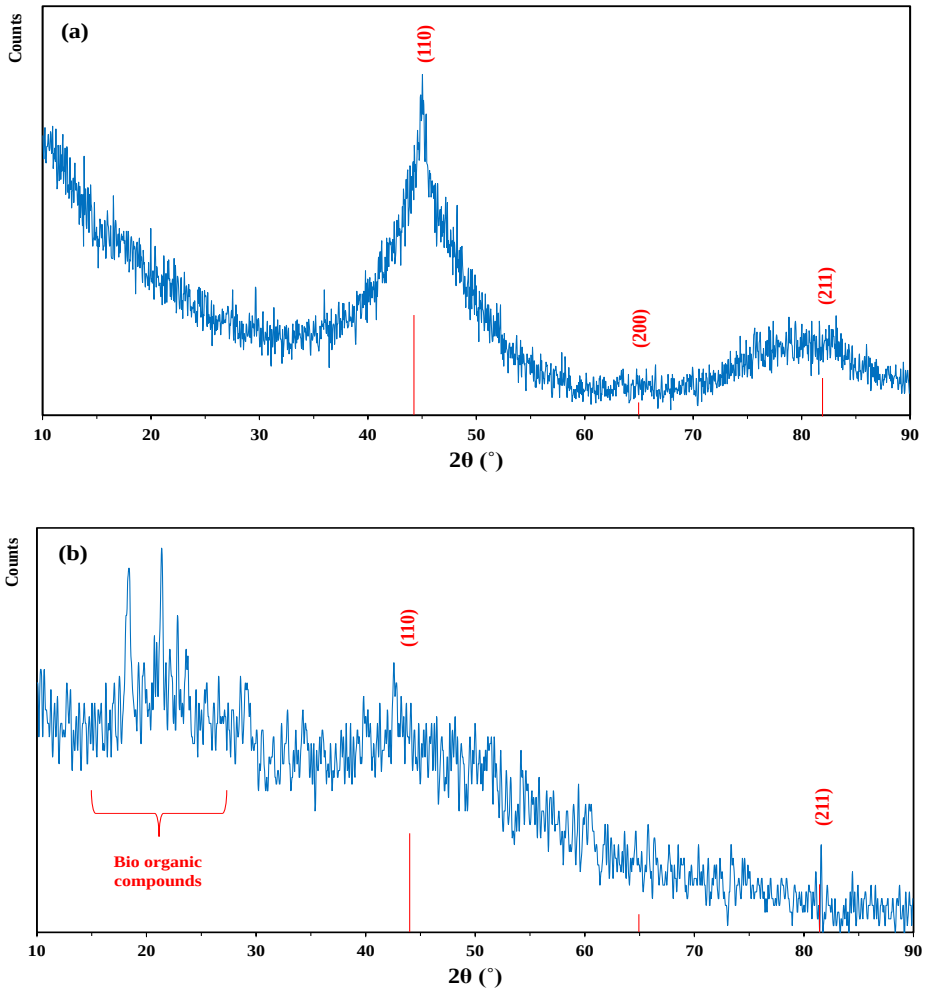

Fig. 2. XRD pattern of the synthesized zero-valent iron nanoparticle by (a) chemical synthesis and (b) biosynthesis method.

These results are similar to the results of the synthesis of zero-valent iron nanoparticles with three plants: *Thymus vulgaris*, *Rosa damascene*, and *Urtica dioica* by Fazlzadeh et al. [34]. They reported that scanning electron microscopy images showed the synthesized nanoparticles were not uniform and different shapes and voids were created. There were also some prominent peaks in the XRD that indicated crystalline iron. They also stated that the reflections created belonged to iron oxide (Fe_3O_4 and Fe_2O_3), zero-valent iron, organic matter, and sodium chloride (NaCl). The results of this study are very similar to the synthesis performed using the extract of *Myrtus communis* by Eslami et al. [9]. In their study, the results of the XRD test using the *Myrtus communis* extract to prepare zero-valent iron nanoparticles also showed the irregularity of the particles. The results of the formation of iron oxide nanoparticles using the extract of *Glycosmis mauritiana* by Amutha & Sridhar [35] also showed the amorphous structure and the crystalline nature of the iron particles created.

3.3. Field Emission Scanning Electron Microscope Analysis

The FESEM images of Fe NPs synthesized using the chemical method and biosynthesis method are shown in Fig. 3, which depicts the morphology and distribution of SB-ZVINs (Fig. 3a) and the TC-ZVINs (Fig. 3b), respectively. As can be seen, the SB-ZVINs didn't a specific shape and morphology and were agglomerated. Most of the particles were in the range of 30-60 nm. It can be said that the formed particles themselves are composed of much smaller particles. In general, as the size of nanoparticles decreases, their specific surface area increases. As the specific surface area of the particles increases, their surface energy increases, and the system tends to stick to each other to reduce its energy. As a result, nanoparticles are seen as larger agglomerates. Comparing the observed particle size with the size of the crystals related to this sample using the Scherrer method, it can be said that the synthesized particles are polycrystalline, and each of them is composed of many crystals with smaller sizes.

The FESEM image of the TC-ZVINs is presented in Fig. 3b and is obvious that the particles appear spherical with a diameter ranging between 40 and 80 nm. Synthesized the TC-ZVINs were dispersed and capped by *T. carmanicus*. Additionally, a decrease in the aggregation of Fe NPs and more singular spherical nanoparticles appearing on the *T. carmanicus* extract was observed. Polyphenols or antioxidants in *T. carmanicus* probably play an important role in controlling the aggregation of the nanoparticles and improving their dispersion by acting as a capping agent. The leaves with high antioxidant capacity and phenolic contents [36, 37] could be a proper candidate for synthesizing different metal nanoparticles with uniform size.

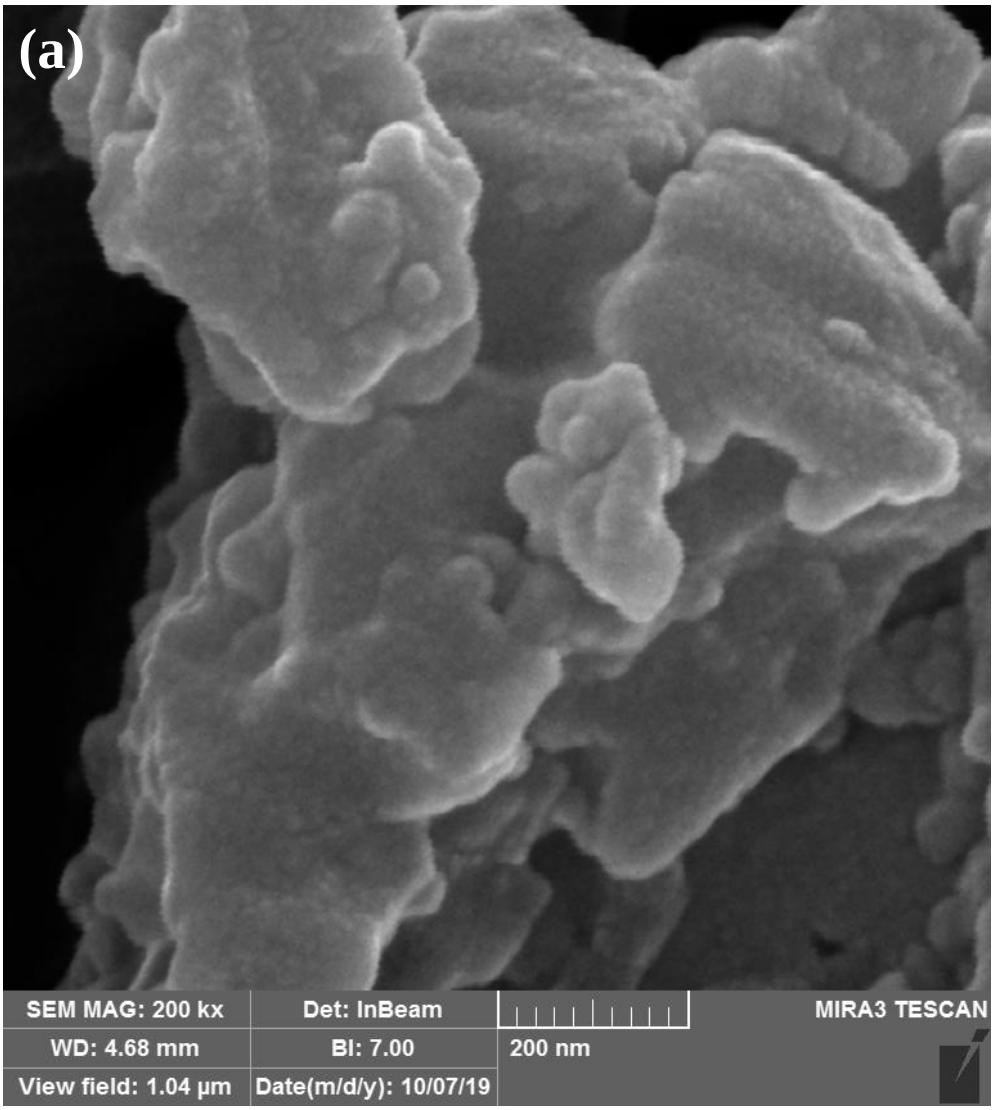

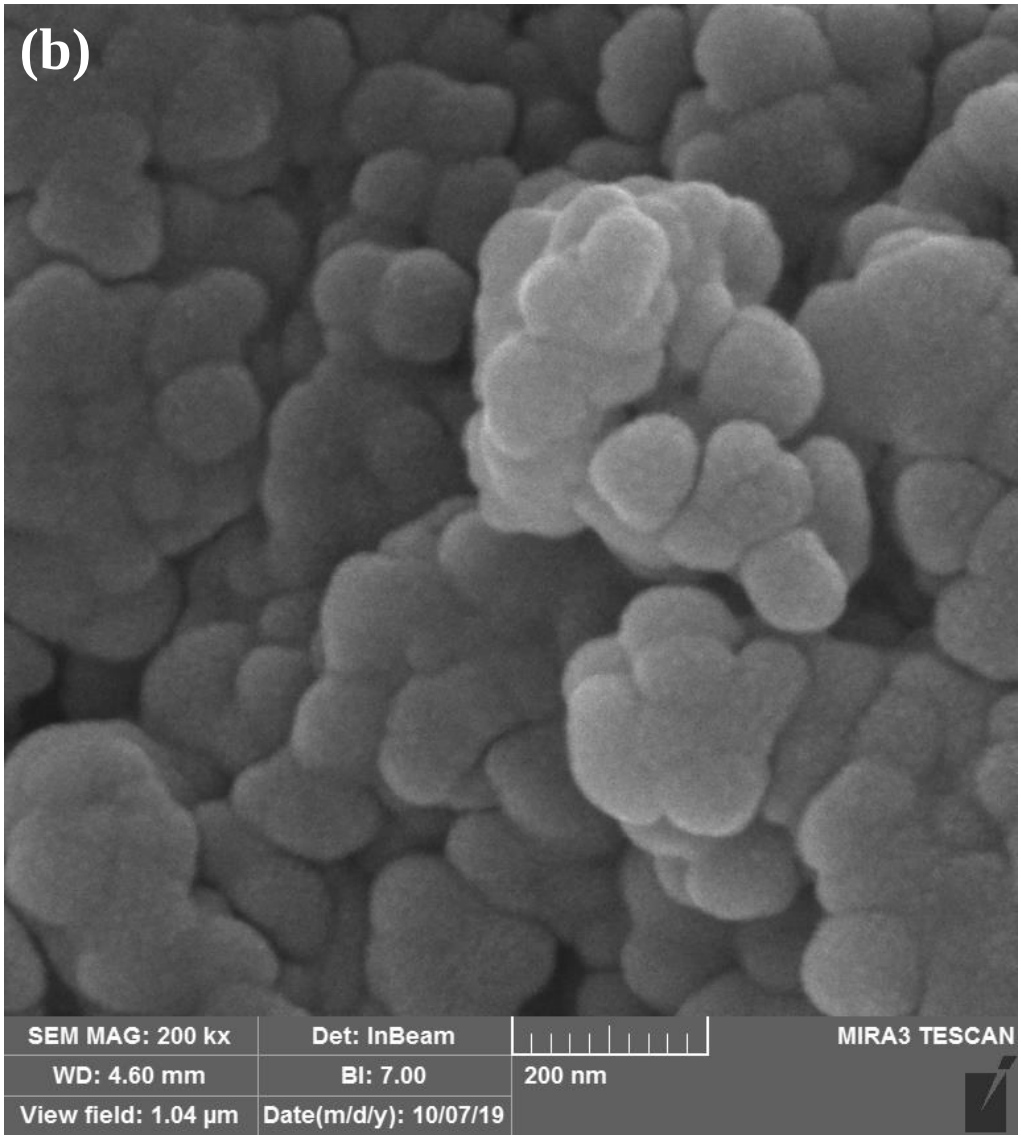

Fig. 3. FESEM images of Fe NPs synthesized using (a) chemical method and (b) biosynthesis method.

3.4. FTIR analysis

FTIR analysis was performed on *T. carmanicus* extract and nanoparticles synthesized by this extract to identify the biological molecules in *T. carmanicus* extract that are responsible for reducing and stabilizing Fe^{3+} ions. FTIR is an analytical technique that measures the intensity of infrared absorption by matter. Figs. 3a and 3b show the FTIR spectrum of *T. carmanicus* extract and zero-valent iron obtained from reaction with *T. carmanicus* extract in the range of 400 cm^{-1} to 4000 cm^{-1}, respectively. Fig. 4a shows intense bands in 3423.7 cm^{-1} (tensile vibrations O-H), 2921.5 cm^{-1} (bending vibrations of aliphatic hydrocarbons C-H and CH_2), 1691.3 cm^{-1} (tensile vibrations C=O), 1606.41 cm^{-1} (tensile vibrations C=C), 1452.14 cm^{-1} (tensile vibrations O-H), and 1051.1 cm^{-1} (deformation O-H). FTIR spectrum of zero-valent iron nanoparticles (Fig. 4b) showed intense bands in 3404.7 cm^{-1} (tensile vibrations O-H), 2925.4 and 2854.1 cm^{-1} (bending vibrations C-H and CH_2 of aliphatic hydrocarbons), 1627.6 cm^{-1} (tensile vibrations C=C), 1350.1 cm^{-1} (tensile C-O of ester group), and 1048.3 cm^{-1} (deformation O-H), as well as absorption bands 816.7 cm^{-1} and 656.6 cm^{-1}, which refers to Fe-O tensions.

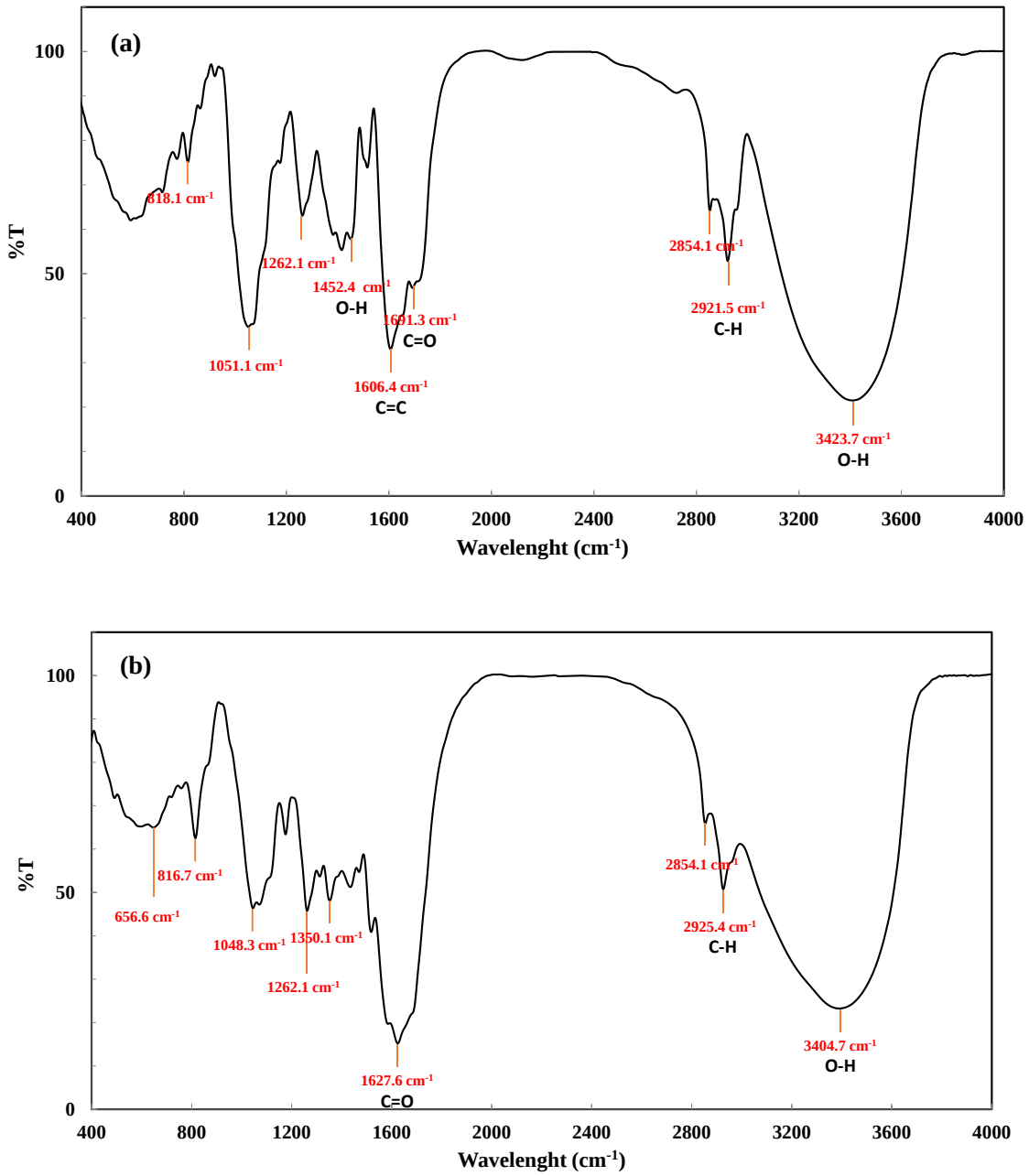

Fig. 4. FTIR spectrum of (a) T. carmanicus extract and (b) T. carmanicus extract stabilized zero valent iron nanoparticles.

By comparison of FTIR spectrum of *T. carmanicus* extract and zero-valent iron nanoparticles obtained from this extract, the band change from frequency 3423.7 cm^{-1} to 3404.7 and from 2921.5 cm^{-1} to 2925.4 cm^{-1} indicates the possible relationship of polyphenolic compounds in the extract (mainly rosmarinic and caffeic acid) in the reduction process through the hydroxyl group and binding to zero-valent nanoparticles through the carbonyl groups. The presence of biochemical molecules in the vicinity of the iron nucleus is probably due to its paramagnetic effects. Spectroscopic analysis of nanoparticle synthesis using three plants *Thymus vulgaris*, *Urtica dioica* and *Rosa damascena* by Fazlzadeh et al. [34] also showed the existence of functional groups of polyphenols and carboxyl as well as proteins and an organic acid which minimizes the density of nanoparticles and is mentioned as a reducing agent. They reported that the highest peak was also attributed to polyphenols, which have shown a strong reduction capacity in plant extracts used [34]. Similar results of the formation of zero-valent iron nanoparticles using the *Myrtus communis* extract by Eslami et al. [9] confirm this. They reported that the possible mechanism in the reduction and stabilization of zero-valent iron nanoparticles by plant extracts can be hydrolyzed by their major constituents, namely phenols. These phenols are hydrolyzed under alkaline conditions (pH =12) and converted to allelic acid, gallic acid, and glucose.

Besides, gallic acid and allelic acid, in their anionic form, could donate electrons and convert them to quinone. This change reduces the iron salt to zero-valent iron. On the other hand, glucose can only reduce Fe^{3+} to Fe^{2+}, the resulting Fe^{2+} being converted to Fe^0 by other anionic forms of hydrolyzed products. Oxidized polyphenols act as a good coating/stabilizing agent in the synthesis and dispersion of zero-capacity iron nanoparticles, which contributes to their stability. Reduction and stabilization by hydrolyzed products of phenols are also supported by the soft and hard acids and bases. The hydroxyl group (-OH) is a hard ligand, while the carbonyl group (-C=O) is a soft ligand. It has already been shown that hard ligands tend to reduce soft metals and soft ligands tend to reduce hard metals. Therefore, when the hard ligand (-OH) in the hydrolysis products of phenols collides with soft metal iron, the Fe^{3+} and Fe^{2+} ions are converted to Fe^0, and the hydrolyzed products of the phenols undergo oxidation to form the quinine forms. The carbonyl group (-C=O) in the form of quinine (IV, V, VI) is a soft ligand that aligns with Fe^0 through electrostatic interactions and helps to stabilize Fe^0 by stopping its growth [9].

3.5. Antibacterial activity for the TC-ZVINs and T. *carmanicus* extract

Qualitative evaluation of the antibacterial performance of the TC-ZVINs and *T. carmanicus* extract and different percentages of them was examined with inhibition zone for 24 h by *Escherichia coli* and *Staphylococcus aureus* using the standard disc diffusion method (Fig. 5a and 5b). The values of growth inhibition zones are presented in Fig. 6. The diameter of the inhibition zone in the TC extract was equal to 8.0 mm and in the TC-ZVINs was equal to 10.7 mm in *Escherichia coli* as a gram-negative bacterium. In general, the diameter of the inhibition zone in TC extract and the TC-ZVINs increased. This diameter was 7.5 mm at a concentration of 20% of the TC-ZVINs, 7.8 mm at a concentration of 40% of the TC-ZVINs, 9.5 mm at a concentration of 60% of the TC-ZVINs and then a slight decrease at a concentration of 80% the TC-ZVINs to 9.8 and finally at a concentration of 100% reached to 10.7. In the gram-positive *Staphylococcus aureus*, the diameter of the inhibition zone in TC extract was 9.0 mm and then it reached 7.8, 8.8, 9.8 and 9.9 by increasing the concentration of the TC-ZVINs at concentrations of 20, 40, 60 and 80. This diameter again increased at a concentration of 100% of the TC-ZVINs and reached 10.8 mm.

The TC-ZVINs and TC extract and different percentages of them have been shown to have antibacterial activity against the tested pathogens. This indicates the potential source of these particles for antibacterial therapy. However, the results of antibacterial tests at different percentages of the presence of nanoparticles do not show much difference in the diameter of the inhibition zone.

In a study conducted by [38] on the antibacterial effect of 4 gram-positive and gram-negative bacteria, including the bacteria used in this study, the inhibition zone of iron nanoparticles was reported 10-17 mm. They reported that FeNPs have great potential due to their antibacterial activity. The antibacterial experiments related to FeNPs are almost similar to the results of Jeyasundari et al. [39]. In a study conducted by [40] on the antibacterial effect of seven gram-positive and gram-negative bacteria, including the bacteria used in this study, inhibition zone values for bacterial strains, which were sensitive to the essential oil of T. *caramanicus*, were in the range of 15–36 mm. They reported that the essential oil of T. *caramanicus* showed high activity against all tested bacteria. The results of this research, with a slight decrease in antibacterial activity, are consistent with our study that has been done using T. *caramanicus* extract. This can be interpreted in another way: first, the presence of the extract in the formed particles, or coincidentally, the antibacterial effects on this nanoparticle and extracts are not much different.

Reports published showed that the antibacterial potential of green synthesized NPs depends on the size of the NPs and the ease with which NPs are released as ions for interaction with bacterial membranes [41, 42]. In our case, the release of the TC-ZVINs as ions might have become difficult as the TC-ZVINs that were prepared were heavily coated with polyphenols. On the other hand, the variation in the shape of as-prepared TC-ZVINs might be one of the factors for the lesser antibacterial potential, as the no uniform-shaped NPs might not have effectively diffused into the bacterial membrane. Another the factor might also be due to the larger size of the TC-ZVINs because larger-sized NPs probably could not manage to diffuse into the bacterial membrane as smaller-sized NPs are found to be more toxic and easier to be uptaken by bacterial membranes [41]. Therefore, the lower antibacterial potential of the TC-ZVINs might be due to their irregular shape and size and the slow release of the TC-ZVINs as ions. Although the TC-ZVINs have exhibited less antibacterial potential, it is at least ascertained that NPs, as synthesized by this route, do have some antibacterial potential. Further research has to be undertaken to modify such zero-valent NPs to enhance their antibacterial potential.

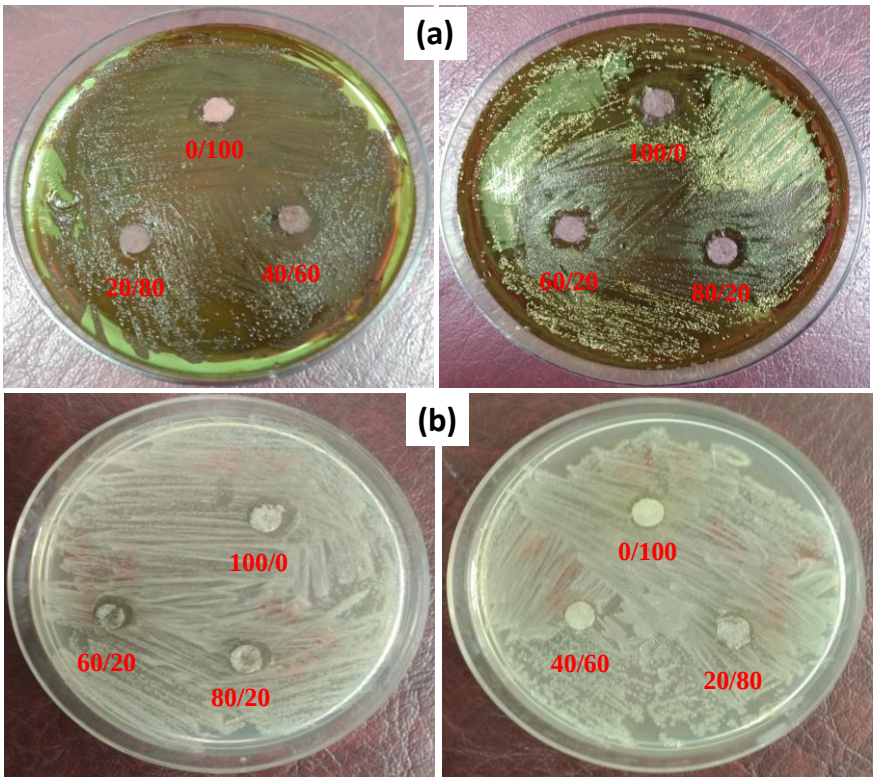

Fig. 5. Images of inhibition zones of the TC-ZVINs and *T. carmanicus* extract samples and different percentages of them after 24 h for (a) *E. coli* and (b) *S. aureus* by the standard disc diffusion method.

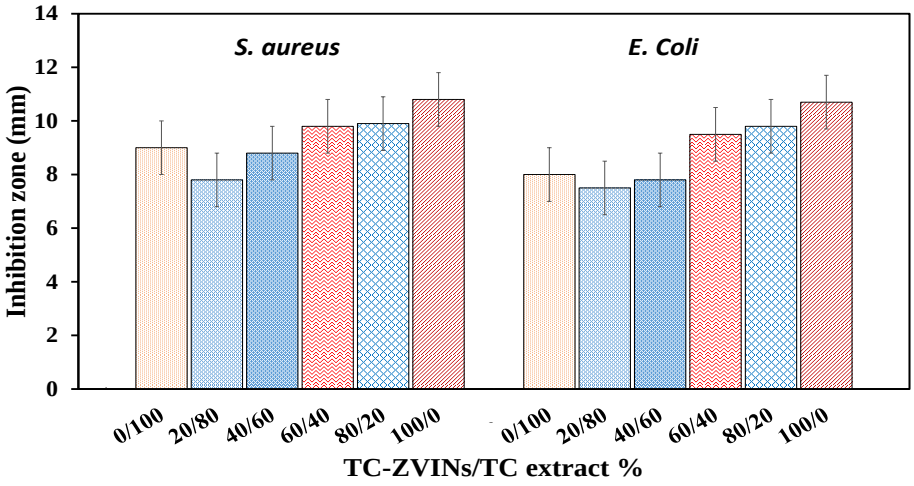

Fig. 6. Values of growth inhibition zones of the TC-ZVINs and *T. carmanicus* extract samples and different percentages of them after 24 h for *E. coli* and *S. aureus* by the standard disc diffusion method.

4. Conclusions

An innovative and promising green synthesis of iron nanoparticles using hydrolyzable polyphenols identified in Thymus carmanicus is reported for the first time. The hydrolyzable polyphenols present in the solvent extract serve as both reducing and capping/stabilizing agents, thus providing an alternative to chemical methods that inevitably involve the use of unsafe reagents and toxic, expensive organic solvents. The presence of an alkaline environment in the synthesis process increases the solubility of the methanolic extract in water and converts the hydroxyl and carboxylic groups available in tannins to stronger reagents through deprotonation. In the biosynthesis method, there is no such strong distinctive diffraction pattern suggesting that the as-prepared NPs are purely amorphous in nature. Based on the FESEM images, it is found that the average-sized nanoparticles have a diameter of around 40-80 nm. FTIR measurements provided powerful evidence that polyphenols form a coat covering the iron nanoparticles to stabilize and prevent their agglomeration. The results of the antibacterial test also showed the TC-ZVINs and *T. carmanicus* extract are both antibacterial. This property is slightly higher in zero-valent iron particles than in *T. carmanicus* extract.

Acknowledgments
This research has been supported financially by Yazd University.

References
[1] N. Kulkarni, U. Muddapur, " Biosynthesis of Metal Nanoparticles: A Review", Journal of Nanotechnology, Vol 2014, 2014, Article ID 510246.
[2] O. Zuas, A. Kristiani, A. Haryono, "Synthesis of the Nano structured Zinc Oxide Using the Soft template of Cylea barbata miers Extract and its Promising Property for Dye Adsorbent", Journal of Advanced Materials and Processing, Vol.3, No. 1, 2015, pp. 39-50.
[3] M. Yazdan-Bakhsh, M. Nasr-Esfahani, R. Esmaeilzadeh-Kenari, M. Fazel-Najafabadi, " Evaluation of antioxidant properties of Heracleum Lasiopetalum extract in multilayer nanoemulsion with biopolymer coating to control oxidative stability of sunflower oil", J. Food Meas. Charact., Vol 15, 2021, pp. 1014–1023.
[4] S. Supraja, S.M. Ali, N. Chakravarthy, A. Jaya Prakash Priya, E. Sagadevan, M.K. Kasinathan, S. Sindhu, P. Arumugam, " Green Synthesis Of Silver Nanoparticles From Cynodon
Dactylon Leaf Extract", Int. J. Chem. Tech. Vol 5, 2013, pp. 271-277.
[5] S. Jafarirad, S. Poorgholi, " Synthesis of CuO Nanoparticles and Investigation on their Applications in Preparing Hair Color", J. Nanomaterials, Vol 7, No. 22, 2016, pp. 95-103.
[6] S.P. Chandran, M. Chaudhary, R. Pasricha, A. Ahmad, M. Sastry, "Synthesis of Gold Nanotriangles and Silver Nanoparticles Using Aloevera Plant Extract", Biotechnol. Prog. Vol 22, No. 2, 2006, pp. 577-583.
[7] M. Savasari, M. Emadi, MA. Bahmanyar, P. Biparva, " Optimization of Cd (II) removal from aqueous solution by ascorbic acid-stabilized zero valent iron nanoparticles using response surface methodology", J Ind Eng Chem, Vol 21, 2015, pp. 1403-1409.
[8] M. Stefaniuk, P. Oleszczuk, Y. Sik Ok, " Review on nano zerovalent iron (nZVI): From synthesis to environmental applications", Chem. Eng. Technol. Vol 287, 2016, pp. 618-632.
[9] S. Eslami, MA. Ebrahimzadeh, P. Biparva, " Green synthesis of safe zero valent iron nanoparticles by Myrtus communis leaf extract as an effective agent for reducing excessive iron in iron-overloaded mice, a thalassemia model", RSC advances, Vol 8, 2018, pp. 26144-26155.
[10] B. Mokhtari, M. Jamzad, F. Falak, " Green Synthesis of Iron oxide Nanoparticles by Using the Aqueous Extract of Melia azedarach L. Leaves and Their Application in "Acid-red 58" Dye Removal from Aqueous Solutions", Journal of Nano Materials, Vol. 14, No. 50, 2022, pp. 89-99.
[11] L. Huang, X. Weng, Z. Chen, M. Megharaj, R Naidu, " Green synthesis of iron nanoparticles by various tea extracts: comparative study of the reactivity", Spectrochim. Acta, Part A Vol. 130, 2014, pp. 295-301.
[12] C.P. Devatha, A.K. Thalla, S.Y. Katte, " Green synthesis of iron nanoparticles using different leaf extracts for treatment of domestic waste water", J. Clean. Prod. Vol. 139, 2016, pp. 1425-1435.
[13] Rechinger KH and Hedge IC 1982 Flora Iranica 150.
[14] D. Sarfaraz, M. Rahimmalek, G. Saeidi, "Polyphenolic and molecular variation in Thymus species using HPLC and SRAP analyses", Sci. Rep. Vol. 11, 2021, pp. 5019.
[15] M. Zare, K. Namratha, M.S. Thakur, K. Byrappa, "Biocompatibility Assessment and Photocatalytic Activity of Bio-hydrothermal Synthesis of ZnO Nanoparticles by Thymus vulgaris Leaf Extract", Materials Research Bulletin, Vol. 109, 2019, pp. 49-59.
[16] M. Hamelian,Mohammad, M. Zangeneh, A. Amisama, K. Varmira, H. Veisi, "Green synthesis of silver nanoparticles using Thymus kotschyanus extract and evaluation of their antioxidant, antibacterial and cytotoxic effects", Applied Organimetalic Chemistry, Vol. 32, No. 9, 2018, e4458.
[17] S.S. Handa, S.P.S. Khanuja, G. Longo and D.D. Rakesh, "Extraction Technologies for Medicinal and Aromatic Plants", (1stedn), no. 66. Italy: United Nations Industrial Development Organization and the International Centre for Science and High Technology, 2008, pp.747-752.
[18] L. Lu, Z. Ai, J. Li, Z. Zheng, Q. Li, L. Zhang, " Synthesis and Characterization of Fe−Fe2O3 Core−Shell Nanowires and Nanonecklaces", Crystal Growth & Design, Vol. 7, No. 2, 2007, pp. 459–464.
[19] B. Moon, Y. Park and K. Park, Fenton oxidation of Orange II by pre-reduction using nanoscale zero-valent iron, Desalination, Vol. 268, Issues 1–3, 2011, pp. 249-252.
[20] C. Zhang, L. Zhou, J. Yang, X. Yu, Y. Jiang, M. Zhou, Nanoscale zero-valent iron/AC as heterogeneous Fenton catalysts in three-dimensional electrode system, Environmental Science and Pollution Research, Vol. 21(14), 2014, pp. 8398-8405.
[21] A. Remmal, T. Bouchikhi, K. Rhayour, M. Ettayebi, A. Tantaoui-Elaraki, Improved Method for the Determination of Antimicrobial Activity of Essential Oils in Agar Medium, Journal of Essential Oil Research, Vol. 5(2), 1993, pp. 179-184.

[22] M.N. Nadagouda, A.B. Castle, R.C. Murdock, S.M. Hussain, R.S. Varma, In vitro biocompatibility of nanoscale zerovalent iron particles (NZVI) synthesized using tea polyphenols, Green Chem. Vol. 12, 2010, pp. 114-122.
[23] M.A. Ebrahimzadeh, F. Pourmorad, A.R. Bekhradnia, Iron chelating activity, phenol and flavonoid content of some medicinal plants from Iran, African Journal of Biotechnology, Vol. 7(18), 2008, pp. 3188-3192.
[24] M.R. Shams Ardekani, M. Khanavi, M. Hajimahmoodi, M. Jahangiri, A. Hadjiakhoondi, Comparison of Antioxidant Activity and Total Phenol Contents of some Date Seed Varieties from Iran, Iran J Pharm Res. Vol. 9(2), 2010, pp. 141–146.
[25] S. Barua, R. Konwarh, S.S. Bhattacharya, P. Das, K.S.P. Devi, T. K. Maiti, M. Mandal, N. Karak, Non-hazardous anticancerous and antibacterial colloidal 'green' silver nanoparticles, Colloids Surf. B, Vol. 105, 2013, pp. 37-42.
[26] G. Ghodake, S.R. Lim, D.S. Lee, Casein hydrolytic peptides mediated green synthesis of antibacterial silver nanoparticles, Colloids Surf., B, Vol. 108, 2013, pp. 147-151.
[27] F. Zhu, S. Ma, T. Liu, X. Deng, Green synthesis of nano zero-valent iron/Cu by green tea to remove hexavalent chromium from groundwater, J. Cleaner Prod. Vol. 174, 2018, pp. 184-190.
[28] X. Weng, L. Huang, Z. Chen, M. Megharaj, R. Naidu, Synthesis of iron-based nanoparticles by green tea extract and their degradation of malachite, Ind. Crops Prod. Vol. 51, 2013, pp. 342-347.
[29] L. Huang, X. Weng, Z. Chen, M. Megharaj, R. Naidu, molecular and biomolecular spectroscopy synthesis of iron-based nanoparticles using oolong tea extract for the degradation of malachite green, Spectrochim. Acta, Part A Vol. 117, 2014, pp. 801-804.
[30] T. Wang, X. Jin, Z. Chen, M. Meghraj, R. Naidu, Green synthesis of Fe nanoparticles using eucalyptus leaf extracts for treatment of eutrophic wastewater, Sci. Total Environ. Vol. 466, 2014, pp. 210-2014.
[31] M. Kamranifar, A. Allahresani, A. Naghizadeh, Synthesis and characterizations of a novel CoFe2O4@CuS magnetic nanocomposite and investigation of its efficiency for photocatalytic degradation of penicillin G antibiotic in simulated wastewater, J. Hazard. Mater. Vol. 366, 2019, pp. 545-555.
[32] A. Alshehri, M.A. Malik, Z. Khan, S.A.A. Thabaiti, N. Hasan, Biofabrication of Fe nanoparticles in aqueous extract of Hibiscus sabdariffa with enhanced photocatalytic activities, RSC Adv. Vol. 7, 2017, pp. 25149-25159.
[33] H. Dong, F. Zhao, G. Zeng, L. Tang, C. Fan, L. Zhang, Y. Zeng, Q. He, Y. Xie, Y. Wu, Aging study on carboxymethyl cellulose-coated zero-valent iron nanoparticles in water: Chemical transformation and structural evolution, Journal of hazardous materials, Vol. 312, 2016, pp. 234-242.
[34] M. Fazlzadeh, K. Rahmani, A. Zarei, H. Abdoallahzadeh, F. Nasiri, R. Khosravi, A novel green synthesis of zero valent iron nanoparticles (NZVI) using three plant extracts and their efficient application for removal of Cr(VI) from aqueous solutions, Advanced Powder Technology, Vol. 28(1), 2017, pp. 122-130.
[35] S. Amutha, S. Sridhar, Green synthesis of magnetic iron oxide nanoparticle using leaves of Glycosmis mauritiana and their antibacterial activity against human pathogens, Journal of Innovations in Pharmaceutical and Biological Sciences, Vol. 5, 2018, pp. 22-26.
[36] W. A. Wannes, B. Mhamdi, J. Sriti, M. B. Jemia, O. Ouchikh, G. Hamdaoui, M. E. Kchouk, B. Marzouk, Antioxidant activities of the essential oils and methanol extracts from myrtle (Myrtus communis var. italica L.) leaf, stem and flower, Food Chem. Toxicol., Vol. 48, 2010, pp. 1362-1370.
[37] V. Smuleac, R. Varma, S. Sikdar, D. Bhattacharyyaa, Green synthesis of Fe and Fe/Pd bimetallic nanoparticles in membranes for reductive degradation of chlorinated organics, J. Membr. Sci. Vol. 379, 2011, pp. 131-137.
[38] J. Das, S. Sankar Dhar, Camellia sinensis mediated synthesis of zero valent iron nanoparticles and study of their efficacy in dye degradation and antibacterial activity, International Journal of Environmental Analytical Chemistry, Vol. 102(18), 2022, pp. 7241-7254.
[39] J. Jeyasundari, P. Shanmuga Praba, Y. Brightson Arul Jacob, V. S. Vasantha, V. Shanmugaiah, Green synthesis and characterization of zero valent iron nanoparticles from the leaf extract of Psidium guajava plant and their antibacterial activity, Chem Sci Rev Lett, Vol. 6(22), 2017, pp. 1244.
[40] S. Nejad Ebrahimi, J. Hadian, M.H. Mirjalili, A. Sonboli, M. Yousefzadi, Essential oil composition and antibacterial activity of Thymus caramanicus at different phenological stages, Food Chemistry, Vol. 110, 2008, pp. 927-931.
[41] Q. Sun, X. Cai, J. Li, M. Zheng, Z. Chen, C.P. Yu, Green synthesis of silver nanoparticles using tea leaf extract and evaluation of their stability and antibacterial activity, Colloids Surf. A. Vol. 44, 2014, pp. 226-231.
[42] A. Singh, P. Kumar Gautam, A. Verma, V. Singh, P. M. Shivapriya, S. Shivalkar, A. Kumar Sahoo, S. Kumar Samanta, Green synthesis of metallic nanoparticles as effective alternatives to treat antibiotics resistant bacterial infections: A review, Biotechnology Reports, Vol. 25, 2020, pp. e00427.